Available online at www.sciencedirect.com
ScienceDirect
Solar Energy 84 (2010) 1852–1862
SOLAR ENERGY
www.elsevier.com/locate/solener

Trends in solar radiation in NCEP/NCAR database and measurements in northeastern Brazil

Vicente de Paulo Rodrigues da Silva [a,*], Roberta Araújo e Silva [a], Enilson Palmeira Cavalcanti [a], Célia Campos Braga [a], Pedro Vieira de Azevedo [a], Vijay P. Singh [b], Emerson Ricardo Rodrigues Pereira [a]

[a] Federal University of Campina Grande/Center of Technology and Natural Resources/Academic Unity of Atmospheric Sciences, Av. Aprígio Veloso, 882, Bodocongó, 58109 970, Campina Grande, PB, Brazil
[b] Dept. of Biological and Agricultural Engineering, Texas A&M Univ., TX 77843-2117, USA

Received 20 November 2009; received in revised form 12 July 2010; accepted 16 July 2010
Available online 23 August 2010

Communicated by: Associate Editor Christian Gueymard

Abstract

The database from the National Center for Environmental Prediction/National Center for Atmospheric Research (NCEP/NCAR) re-analysis project available for the period from 1948 to 2009 was used for obtaining long-term solar radiation for northeastern Brazil. Measurements of global solar radiation (R_s) from data collection platform (DCP) for four climatic zones of northeastern Brazil were compared to the re-analysis data. Applying cluster analysis to R_s from database, homogeneous sub-regions in northeastern Brazil were determined. Long times series of R_s and sunshine duration measurements data for two sites, Petrolina (09°09′S, 40°22′W) and Juazeiro (09°24′S, 40°26′W), exceeding 30 years, were analyzed. In order to exclude the decadal variations which are linked to the Pacific Decadal Oscillation, high-frequency cycles in the solar radiation and sunshine duration time series were eliminated by using a 14-year moving average, and the Mann–Kendall test was employed to assess the long-term variability of re-analysis and measured solar radiation. This study provides an overview of the decrease in solar radiation in a large area, which can be attributed to the global dimming effect. The global solar radiation obtained from the NCEP/NCAR re-analysis data overestimate that obtained from DCP measurements by 1.6% to 18.6%. Results show that there is a notable symmetry between R_s from the re-analysis data and sunshine duration measurements.

Keywords: Global dimming; Mann–Kendall test; Net radiation; Pacific Decadal Oscillation

1. Introduction

Solar radiation drives almost all physical, chemical and biological processes in the earth's atmospheric system. Long-term trends in solar radiation have received an increasing attention due to its large influence on the hydrological cycle. Using a deterministic radiation transfer model and data from NCEP/NCAR re-analysis, Hatzidimitriou et al. (2004) determined a decadal increase in the outgoing longwave radiation at the top of the atmosphere. Others studies have also shown a mix (increasing and decreasing) of statistically significant trends in outgoing longwave radiation at the top of the atmosphere (Chen et al., 2002) and surface reflected solar radiation (Tashima and Hartmann, 1998). The average amount of sunlight reaching the ground has been decreasing in some parts of the world (Liepert and Kukla, 1997; Liepert, 2002). Otherwise, several studies have suggested that the increasing trend of approximately 0.5–0.7 °C in global temperature over the last century may have solar origin (Abakumova et al., 1996; Fotiadi et al., 2005). The "global dimming"

* Corresponding author. Tel./fax: +55 8333101202.
E-mail address: vicente@dca.ufcg.edu.br (V.P.R. Silva).

0038-092X/$ - see front matter
doi:10.1016/j.solener.2010.07.011

effect refers to observed reduction in solar radiation reaching the earth's surface in the last 50 years in some places of the world, and it suggests several consequences as regards climate, particularly the hydrological cycle (Nazarenko and Menon, 2005). The NCEP/NCAR re-analysis project provides daily data (1948-present) of several atmospheric variables, including solar radiation (Kalnay et al., 1996). These data can be used for assessing climate variability which is perhaps the greatest threat to life on Earth.

A major source of inter-annual climate variations in several parts of the globe is the El Niño/Southern Oscillation (ENSO) (Kayano and Andreoli, 2007). For example, the ENSO cycle explains a large part of the inter-annual rainfall variability in South America (Grimm, 2003; Vera et al., 2004). On the other hand, Kayano and Andreoli (2004) reported that the decadal variations (9–14 year) of the northern NEB (northeastern Brazil) rainfall are linked to the Pacific Decadal Oscillation (PDO) or to the sea surface temperature (SST) decadal variations in the tropical South Atlantic (TSA). Obviously, decadal cycles observed in rainfall over northeastern Brazil are closely associated with variation in cloudiness which therefore impacts solar radiation. Decadal-scale fluctuations are crucial particularly to northeastern Brazil, because they control water supplies and may modulate higher frequency events such as floods and droughts. The presence of various motion scales in time series may complicate the analysis and interpretation of long-term trends of meteorological variables. Thus, the cycles must be accurately removed before performing statistical tests, which require that the data be statistically independent and identically distributed for detecting long-term trends (Eskridge et al., 1997).

Since the solar renewable energy community has long depended upon solar radiation measurements (Gueymard and Myers, 2009), the knowledge of solar resource at the earth surface, with enough accuracy, is essential for planning any solar energy system at a given location (Zarzalejo et al., 2009). However, the necessary equipments for solar energy measurements are available only at a few places. As a consequence, many models for estimation of solar radiation have been developed as a function of other climatic variables, such as sunshine duration (El-Metwally, 2004; Chineke, 2008; Bakirci, 2009). On the other hand, solar radiation derived from satellite images or re-analysis data can be advantageous for characterization of solar resource over large areas. In addition, a stochastic model based on cloudiness observations for simulating global solar radiation on a horizontal surface has also been developed (Ehnberg and Bollen, 2005).

One of the main limitations of the methods, based on meteorological data, that are commonly available is that they require calibration using on-site measurements of solar radiation data and it is therefore open to question how transferable these calibration values are to other locations. Obviously, measured data is the best form of this knowledge; however, there are very few meteorological stations with measurement of global solar radiation, particularly in developing countries (El-Metwally, 2005). A large number of studies on changes in solar radiation and sunshine duration have been also published (Power and Goyal, 2003; Liu et al., 2004; Power and Mills, 2005). Despite all of these studies, there is very scarce information on global dimming effect in Brazil. This effect has received limited attention and it is thus poorly understood. The objective of this study is to assess trends in solar radiation in northeastern Brazil using the NCEP/NCAR database and surface measured data; analyze trends in measured global solar radiation and sunshine duration obtained from data collection platform (DCP) by a non-parametric test; analyze the global dimming effect in the region of study; and measure the accuracy of re-analysis data as compared to DCP data using statistical indicators.

2. Data and methods

2.1. Study area

The region chosen for this study is the northeastern Brazil which covers an area of about 1.5 million square kilometers and borders the Atlantic Ocean on the north and east side. The semiarid part of the region is inhabited by more than 30 million people and presents a large variability in both inter-annual and spatial rainfall (Silva, 2004). This area is extremely vulnerable to the combined effects of natural hazards and human activity. Fig. 1 shows the map of northeastern Brazil, including the spatial distribution of the NCEP/

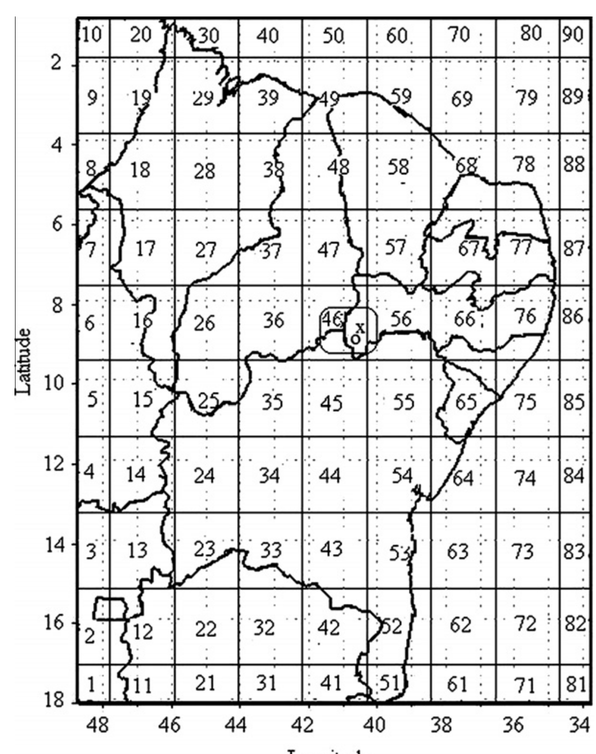

Fig. 1. Spatial distribution of the NCEP/NCAR grid points in a tropical region (1°S–18°S; 33°W–48 W°) with 90-grid points over northeastern Brazil. Each grid point has 2.5° longitude–latitude resolution.

NCAR 90-grid points in a tropical region (1°S–18°S; 33°W–48 W°), as well as the position of two meteorological stations, Petrolina (09°09′S, 40°22′W) and Juazeiro (09°24′S, 40°26′W), on grid point 46 whose data would be discussed. Normal annual rainfall ranges from less than 400 mm in the center of the semiarid region to 1800 mm in the eastern coast. Annual average temperature varies from 16.8 to 33.8°C and evaporation rates can surpass 10 mm d^{-1} (Silva et al., 2006).

2.2. Mann–Kendal test

The World Meteorological Organization (WMO) recommends using the Mann–Kendall non-parametric test (Mann, 1945; Kendall, 1975) for assessing trends in environmental time series data (Yu et al., 2002). This test consists of comparing each value of a time series with the other remaining values in sequential order. The number of times that the remaining terms are greater than that under analysis is counted. This test is based on statistic S defined as:

$$S = \sum_{i=2}^{n}\sum_{j=1}^{i-1}\text{sign}(x_i - x_j) \tag{1}$$

where x_j's are the sequential data values, n is the length of the time series and sign $(x_i - x_j)$ is -1 for $(x_i - x_j) < 0$ for $(x_i - x_j) = 0$, and 1 for $(x_i - x_j) > 0$. The mean $E[S]$ and variance $V[S]$ of statistic S may be given as:

$$E[S] = 0 \tag{2}$$

$$\text{Var}[S] = \frac{n(n-1)(2n+5) - \sum_{p=1}^{q} t_p(t_p - 1)(2t_p + 5)}{18} \tag{3}$$

where t_p is the number of ties for the pth value and q is the number of tied values. The second term represents an adjustment for tied or censored data. The standardized test statistic (Z_{MK}) is computed as:

$$Z_{MK} = \begin{cases} \frac{S-1}{\sqrt{\text{Var}(S)}} & \text{if } S > 0 \\ 0 & \text{if } S = 0 \\ \frac{S+1}{\sqrt{\text{Var}(S)}} & \text{if } S < 0 \end{cases} \tag{4}$$

The presence of a statistically significant trend is evaluated using the Z_{MK} value. This statistic is used to test the null hypothesis that no trend exists. A positive Z_{MK} value indicates an increasing trend, while a negative one indicates a decreasing trend. To test for either increasing or decreasing monotonic trend at the p significance level, the null hypothesis is rejected if the absolute value of Z_{MK} is greater than $Z_{MK1-p/2}$ which is obtained from the standard normal cumulative distribution table. In general, the significance levels of $p = 0.01$ and 0.05 are applied. A non-parametric estimate for the magnitude of the trend slope was obtained as follows (Hirsch et al., 1982):

$$\beta = \text{Median}\left[\frac{(x_j - x_i)}{(j - i)}\right] \quad \text{for all } i < j \tag{5}$$

where x_j and x_i are data points measured at times j and i, respectively.

2.3. Cluster analysis

Cluster analysis refers to a set of techniques designed to classify observations so that members of the resulting groups are similar to each other and distinct from other groups. Hierarchical clustering, which successively joins the most similar observations, is the most common approach (Davis, 1986). Because groups are simply based on their similarity to each other, hierarchical cluster analysis can be useful when abundant data are available. Euclidean distance was used to compute the distance among grids and the clustering procedure used was the average linkage method. This procedure is based on the average distance between all pairs of objects (grids) considering that the two objects must belong to different clusters. The two objects with the lowest average distance are linked to form a new cluster. Cluster analysis technique may also be thought of as a useful way of objectively organizing a large data set into unknown groups on the basis of a given set of characteristics (Gore, 2000). This can ultimately assist in the recognition of potentially meaningful patterns. The set of characteristics chosen for inclusion in the cluster analysis is assumed to include important distinguishing characteristics of the entities that are being clustered. After the cluster analysis, the grouping of input data is detected. The number of clusters and the members belonging to the corresponding cluster are both determined. In this study, cluster analysis was used to obtain groups of relatively homogeneous global solar radiation in northeastern Brazil.

2.4. Performance of re-analysis statistics

To assess whether or not the NCEP/NCAR re-analysis data are appropriate, the goodness-of-fit was tested against most widely used statistical indicators. The mean bias difference (MBD) and the normalized root mean square difference (NRMSD) are obtained as follow (El-Metwally, 2005):

$$\text{MBD} = \sum_{i=1}^{i=n}\frac{(P_i^* - P_i)}{n} \tag{6}$$

$$\text{NRMSD} = \frac{\left[\sum_{i=1}^{i=n}\frac{(P_i^* - P_i)^2}{n}\right]^{1/2}}{\frac{1}{n}\sum_{i=1}^{i=n}P_i} \tag{7}$$

where n is the number of data pairs, P_i^* and P_i are the ith modeled and measured values of monthly mean global solar radiation, respectively.

2.5. Data description

For each grid point as shown in Fig. 1, monthly time series of global solar radiation, shortwave, longwave and net radiation were obtained from NCEP/NCAR re-analysis project for the 1948–2009 period. It is important to recognize that the surface radiative fluxes calculated from NCEP data are mainly determined by clouds and aerosol information has not been used as input for the re-analysis project. Measurements of global solar radiation were obtained by Eppley Precision Spectral Pyranometer (PSP) for the 1975–2009 period at two sites of the semiarid region of northeastern Brazil (Petrolina and Juazeiro). Although these pyranometers are reasonably accurate, they were periodically calibrated against a standard pyranometer at least once a year.

Global solar radiation at grid point 46 derived from re-analysis data was compared to that obtained by averaging the available data in the meteorological stations of Petrolina and Juazeiro. Also, the global solar radiation obtained from DCP for four selected grid points (56, 29, 68 and 65) in northeastern Brazil were compared to the re-analysis data. For groups 1–4, monthly global solar radiation data from DCP were obtained by averaging the data available at two or three weather stations at each grid point and then compared to the NCEP/NCAR data for a period varying from 41 to 60 months. Sunshine duration (or insolation) is defined as the amount of time that direct radiation exceeds a certain threshold, usually taken at 120 W m^{-2}, and can be considered as a proxy measure of global radiation (Stanhill and Cohen, 2001). In the present study, the sunshine duration time series for Petrolina and Juazeiro as well as from DCP were also analyzed.

Fig. 2 shows groups of relatively homogeneous global solar radiation in northeastern Brazil. Two observational sites (Petrolina and Juazeiro) fall in group 1 which covers most of the semiarid region. The northern region (group 2) has a different pattern of solar radiation in comparison to that observed at the northern coast (group 3) and eastern and southeastern coasts (group 4). For instance, annual rainfall decreases across northeastern Brazil from 1500 mm in the eastern to less than 400 in the central and western semiarid region.

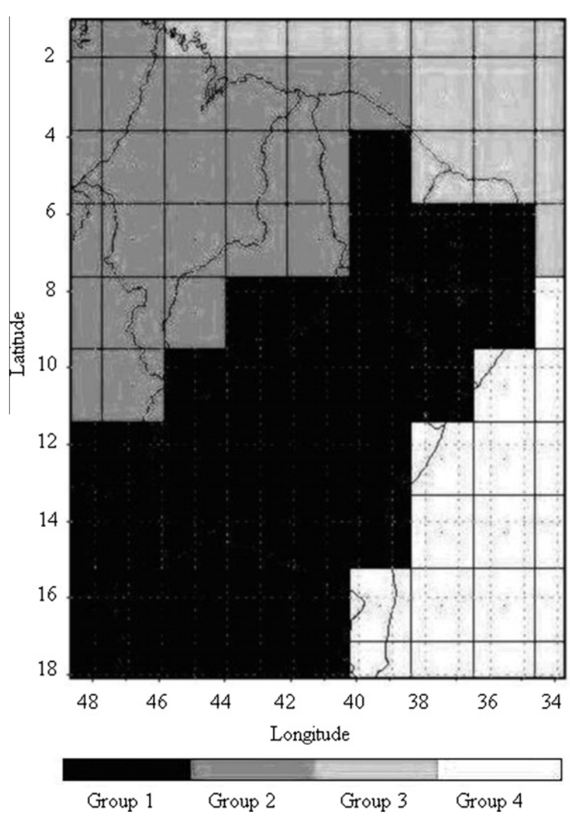

Fig. 2. Geographical positions of global solar radiation groups over northeastern Brazil. Data are from NCEP/NCAR re-analysis project for the 1948–2009 period.

Kayano and Andreoli (2004) observed that the decadal (9–14 years) rainfall variations of the northern part of northeastern Brazil are independently linked to the Pacific Decadal Oscillation (PDO) or to the sea surface temperature decadal variations in the tropical South Atlantic. Likewise, cycles less than 10-year in rainfall time series has been observed in all northeastern Brazil, including the central and southern parts of region, as well as the 11-year cycle which is related to solar activity (P. V. Azevedo, personal communication). Since decadal and multi-decadal cycles observed in rainfall time series are closely associated with cloudiness and thus impacting solar radiation, a 14-year moving average was used for eliminating high-frequency cycles in both solar radiation and sunshine duration time series. The filtered time series of re-analysis and measurements were then subjected to the trend and correlation analyses. The wavelet transform and moving average filter methods are shown to be capable of separating synoptic and seasonal components in time series with minimal errors (Eskridge et al., 1997). The moving average filter method is shown to have the same level of accuracy as the wavelet transform method. However, the moving average can be applied to datasets with missing observations and is much easier to use than the wavelet transform method.

3. Results and discussion

The grid points considered in the study are located in different climatic zones of northeastern Brazil. The databases described in Tables 1–3 were statistically processed and analyzed after the removal from the decadal (<14-year period) variations of both solar radiation and sunshine duration, as described previously.

3.1. Long-term trend in sunshine duration and global solar radiation

The filtered time series of sunshine duration and annual mean daily global solar radiation obtained from re-analysis data showed significant trends for distinct time periods (Fig. 3). Although the data set includes the 1962–2009 per-

Table 1
Geographical locations of stations with sunshine duration data located over corresponding grid point with global solar radiation.

Station	Group	Grid point	Latitude	Longitude
Petrolina	1	46	09°23′55″S	40°30′03″W
Fortaleza	2	59	03°43′02″S	38°32′35″W
João Pessoa	3	76	07°06′54″S	34°51′47″W
Salvador	4	54	12°58′16″S	38°30′39″W

Table 2
Geographical locations of data collection platform stations and the observational period for each group in northeastern Brazil.

Groups	Period of record	Stations	Latitude	Longitude
Group 1	January/2006–December/2009	Serra Talhada	07°59′31″S	38°17′54″W
		Sertânia	08°04′25″S	37°15′52″W
		B. São Francisco	08°45′14″S	38°57′57″W
Group 2	January/2005–December/2009	Pinheiro	02°31′17″S	45°04′57″W
		Urbano Santos	03°12′28″S	43°24′13″W
		São Luís	02°31′47″S	44°18′10″W
Group 3	January/2006–December/2009	Natal	05°47′42″S	35°12′34″W
		Banabuiú	05°18′35″S	38°55′14″W
Group 4	January/2005–May/2008	N. S. da Glória	10°13′06″S	37°25′13″W
		Itabaiana	10°41′06″S	37°25′31″W

Table 3
Summary of statistical performance of the mean monthly global solar radiation (MJ m^{-2} day^{-1}) from NCEP/NCAR re-analysis and DCP[a] data for four select grid points in northeastern Brazil. MBD (MJ m^{-2} day^{-1}) = Mean bias difference, NRMSD (%) = normalized root mean square difference, r^2 = coefficient of determination.

Group	Grid point	MBD	NRMSD	r^2
1	56	−1.11	8.1	0.71
2	29	−0.28	6.3	0.77
3	68	−2.53	16.9	0.49
4	65	−4.25	24.4	0.62

[a] DCP = data collection platform.

iod, it is clear from this figure that the sunshine duration time series refer to the 1974–2009 period. The annual mean daily global solar energy from re-analysis data for four selected grids and measurements of sunshine duration for one representative stations of each group were consistent. The geographical locations of these stations and their both corresponding groups and grid points are shown in Table 1. There is a notable symmetry between re-analysis global solar radiation and sunshine duration measurements. When global solar radiation time series are increasing the sunshine duration time series are decreasing and vice versa, since the amounts of solar radiation received are closely related to the sunshine duration (Wan et al., 2009). This agrees with the fact that one of the most widely adopted climatic parameters to estimate global solar radiation is the possible bright sunshine (Wan et al., 2009).

The global solar radiation time series is increasing at grid points 54, 59 and 76 and decreasing at grid point 46. The physical reason for this is associated with cloudiness of the region. The cloud cover amount in grid point 46 was calculated by averaging the data available at the meteorological stations of Petrolina and Juazeiro. Thus, the sunshine duration increases were caused by the large expansion of the irrigated perimeter over middle reaches of the San Francisco River valley where these two meteorological stations are located. This region is the major tropical fruit production center in Brazil, where more than 100,000 ha are irrigated (Silva et al., 2009). The large amount of water exposed to the atmosphere by irrigation has kept this region with moistened atmospheric air (Silva 2004). Once the re-analysis global solar radiation decreases with increasing cloudiness and vice versa, it is obvious that the re-analysis data are consistent when compared to surface measurements. The global solar radiation at grid points 54, 76 and 59 presented statistically significant trends at $p < 0.01$ according to the Mann–Kendall test while for the grid point 46 they were significant only at $p < 0.05$. On the other hand, significant trends at $p < 0.01$ were observed only for the grids 76 and 59. The largest increase in global solar radiation of 1.26 MJ m^{-2} day^{-1} during the analyzed period was occurring at grid 54.

Decreasing trends in the sunshine duration time series were observed for all grid points except for grid point 46 where a small increase of 0.34 h was observed. An explanation for the increase in sunshine duration at grid point 46 can be greatly attributed to irrigation which leads to an increase in cloud cover while the decreasing trends in global radiation can also be explained by the effect of cloudiness in their optical properties. According to Supit and Van Kappel (1998), clouds and their accompanying weather patterns are among the most important atmospheric phenomena restricting the availability of solar radiation at the earth's surface.

The long-term linear trend in global solar radiation measurements at Petrolina and Juazeiro stations are shown in Fig. 4. For eliminate high-frequency cycles in the time series the data were also smoothed by a 14-year moving average. The two stations are quite close to one another because unfortunately there are very few meteorological stations for measuring global solar radiation in northeastern Brazil. These two stations are located in the semiarid region of northeastern Brazil. Time series in global solar radiation for both meteorological stations showed a decreasing trend statistically significant at the 1% significance level by Mann–Kendall test. Similar results were obtained by Liepert and Kukla (1997) who found a statistically significant decrease in annual mean global solar radiation between 1964 and 1990 under completely overcast skies at five out of eight studied locations in Germany. They observed that the decreasing trend in radiation was probably related to the recovery from the effects of major volcanic eruptions in the mid-1960s and 1980s.

From our study, even for the 1988–2009 period one may note that the solar radiation reduction may be associated with global dimming. This result must however be taken with caution because of the scarcity of long-term observations of solar radiation over the study region. However, previous studies have shown similar reductions in global solar radiation reaching the earth's surface during the last 50 years in other parts of the world (Liepert and Kukla, 1997; Liepert, 2002; Power and Mills, 2005). The most significant decreases in global solar radiation for Juazeiro and

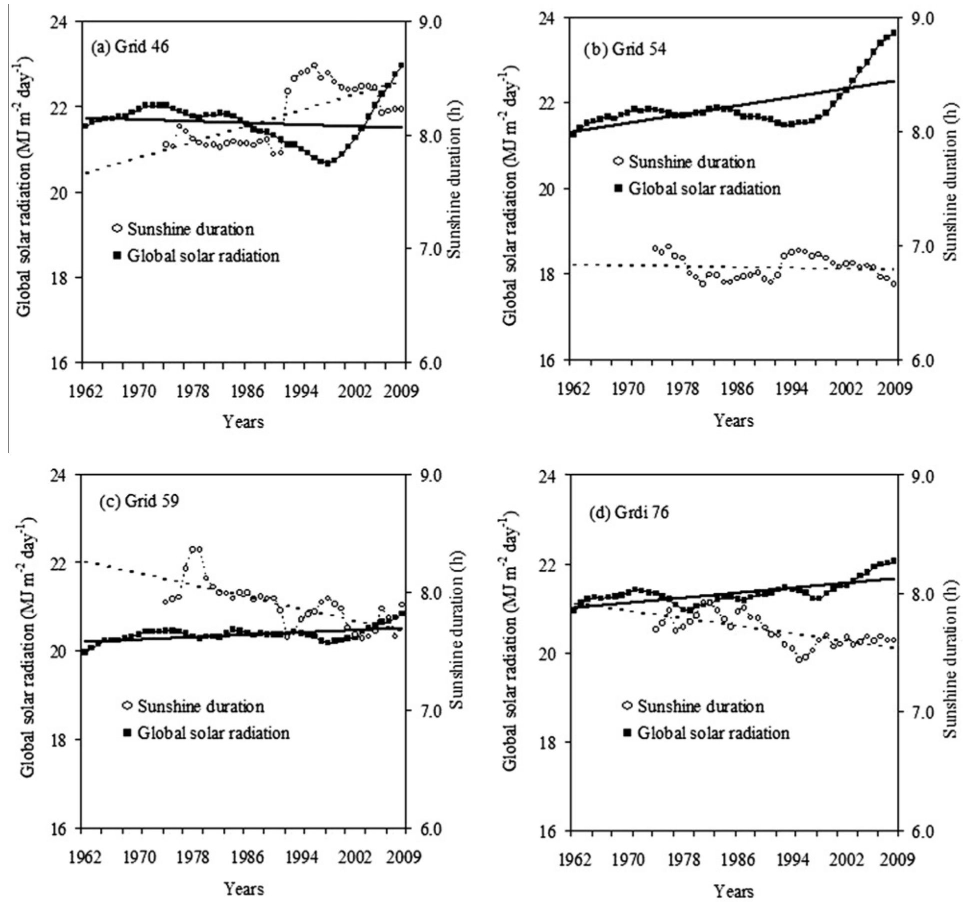

Fig. 3. Long-term trends in global solar radiation (MJ m^{-2} day^{-1}) based on re-analysis data and sunshine duration measurements (hours) for four selected grid points in northeastern Brazil.

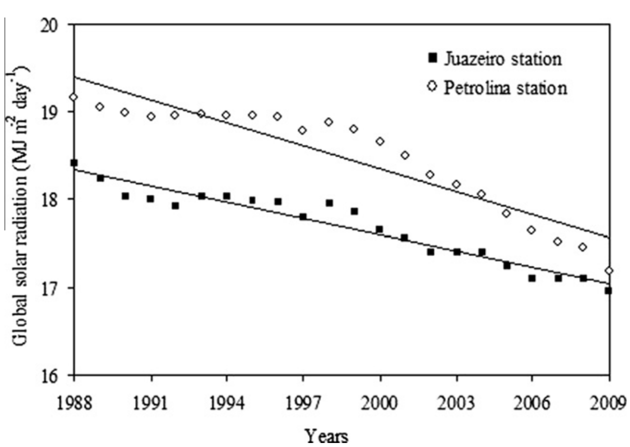

Fig. 4. Long-term trends in observed global solar radiation at Petrolina (09°09′S, 40°22′W) and Juazeiro (09°24′S, 40°26′W) stations, Brazil.

Petrolina stations are 1.36 and 1.93 MJ $m^{-2}day^{-1}$, respectively, corresponding to 7.7% and 10.4% of the average global solar radiation for the whole study period (1988–2009). The observed global solar radiation has fallen since 1988 as the sunshine duration has increased (Fig. 3a). Since the reduction of solar radiation is likely to be caused by increasing cloud cover, the class A pan evaporation and wind speed are also decreasing at both stations (results are not presented). Another effect of decreasing evaporation results from the fact that wind speed plays an important role in this physical process. It is most likely that cloud variations have an important role in the decreasing trends of evaporation and global solar radiation.

3.2. Seasonal solar radiation

The geographical locations of DCP stations and the observed global solar radiation period for each group are shown in Table 2. Since the reliable long-term global solar radiation measurements are scarce, the data were averaged taking into account 2–3 stations as representative for each group. The DCP data varies from 41 to 60 months which were compared to the same temporal resolution of re-analysis global solar radiation data. The average over each group indicates that global solar radiation from NCEP/NCAR re-analysis data overestimates those from DCP by ranging from 1.6% (group 2) to 18.6% (group 4). The global solar radiation from re-analysis data is on average 9% higher than that from DCP data. Similar results were obtained by Lohmann et al. (2006) by comparing solar radiation from NCEP/NCAR re-analysis data with satellite observations.

Distinct seasonal variations of monthly daily mean global solar radiation can be observed for both re-analysis and DCP data with annual peak during summer period (Fig. 5). The global solar radiation from re-analysis data tended to follow that from DCP measurements for each grid point. However, the measurements are always lower than re-analysis data, except for some months at grid point 29. However, the differences between modeled and measured values are negligible. Nevertheless, the highest difference between measurements and re-analysis data was found for grid points 68 (Fig. 5c) and 65 (Fig. 5d) which are located at the east coast of northeastern Brazil. For quantifying the difference and the relationship between values, MBD, NRMSD and r^2 were obtained for each analyzed grid point and a summary is shown in Table 3. Since the value of NRMSD is always positive, representing zero as in the ideal case, the best fit was found for grid point 29, while the worse fit was obtained for grid point 65.

The MBD values are negative for all grid points indicating a 0.28–4.25 MJ m^{-2} day^{-1} underestimation of global solar radiation. On the other hand, NRMSD varied from 6.3% to 24.4% in the northern part and at the east coast of the region, respectively. El-Metwally (2004) found NRMSD for global solar radiation estimated by simple method and by Angstron–Prescott method of about 11–12% at all analyzed sites. The coefficients of determination between NCEP/NCAR re-analysis data and DCP data for central and northern parts of the region were higher than those for the eastern coast. These results also suggest that the estimation errors increase with increasing cloudiness. The cloud cover amount was gradually decreasing from eastern coast to semiarid and northern parts of the region as a consequence of southern cold fronts and eastern upper air cyclonic vortex from Atlantic Ocean. Similar results were obtained by El-Metwally (2005) by analyzing the sunshine and global solar radiation estimation in Egypt. He attributed the increase in errors to the invasion of winter extra-tropical systems from the north crossing over the Mediterranean, causing increases in cloudiness in northern Egypt. Although grid point 68 had a low coefficient of determination (0.49), it showed MBD and NRMSD values lower than those for grid point 65.

Re-analysis data yielded the highest coefficient of determination at grid 29 followed by grid 56. Grid points 65 and 68 which are located in the east coast of the region showed worst coefficient of determination and highest values of NRMSD for both grids. The statistical performance indicated that the re-analysis data are better for central and northern parts of region than for the eastern coast. By designing a hybrid model for estimating monthly mean daily global radiation from hourly-recorded bright sunshine time for Japan, Yang et al. (2001) showed that the cloudy weather condition was one main contributor to the greater errors. Statistical indicators, MBD, NRMSD and r^2, were also used for quantifying the relationship between re-analysis and measurements data. Annual mean

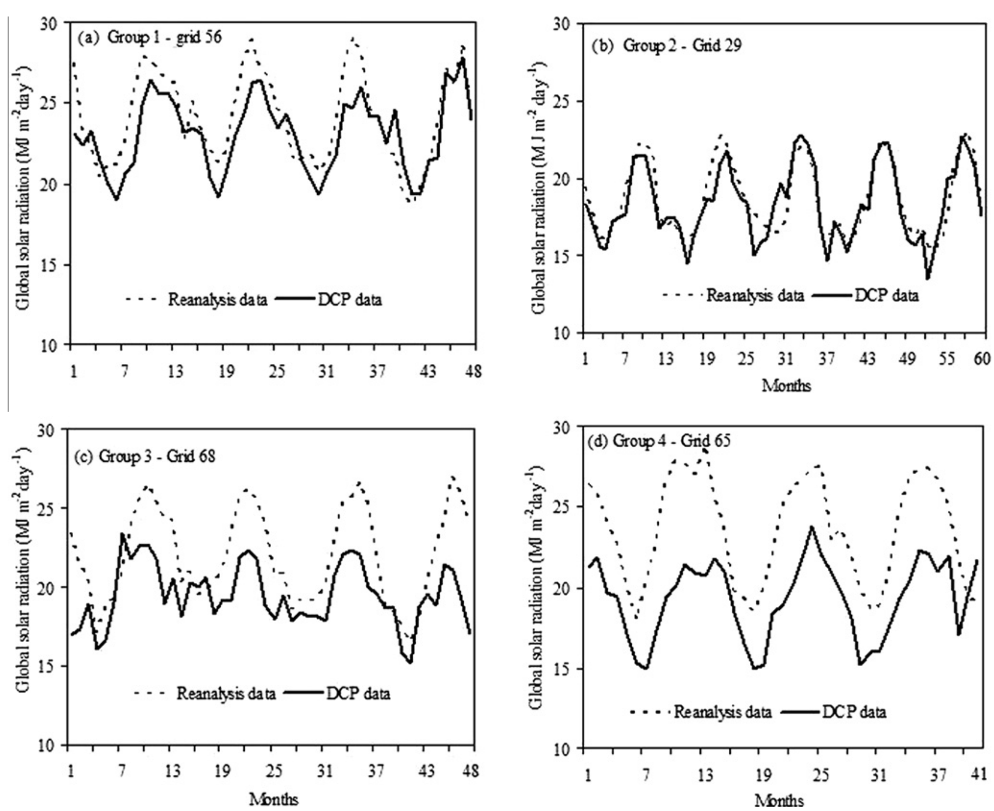

Fig. 5. Comparison of monthly global solar radiation (MJ m^{-2} day^{-1}) from re-analysis and measurements by data collection platform (DCP) for four select grid points in northeastern Brazil.

daily global solar radiation from NCEP/NCAR re-analysis data at grid 46 was compared to that obtained by averaging the data available at the Petrolina and Juazeiro meteorological stations which are located at same grid point.

3.3. Relationship between re-analysis and measured data

The coefficient of determination indicated a strong relationship between modeled and measured annual average daily global solar radiation data (Fig. 6). Comparing the measurements of global radiation values with the predicted values at grid 46, the points were positioned around a straight line. The relationship between data is inverse or negative, since the measured global solar radiation decreases as re-analysis data increases. This reverse relationship may be related to the increase in cloudiness in the region of Petrolina and Juazeiro throughout the year, as previously mentioned. Such a phenomenon may adversely affect the solar radiation derivation in the region. Furthermore, the initial and boundary conditions of the NCAR/NCEP model do not regard the recent changes in the region surface vegetation characteristics. Annual mean of global solar radiation from re-analysis data is higher than measurements by 15.9%. This difference is probably because only two stations were used in the analysis. Also, these stations are either a little representative for the whole area with 2.5 degree grid (≈210 km) or not with the accuracy required by the re-analysis data.

The reductions in solar radiation measurements are higher for measurements than for NCEP/NCAR re-analysis data. This slower reduction in re-analysis data may be possibly due to its low spatial resolution and the lack of aerosols data. Although the surface stations provide reliable surface flux data, the limited number of stations and their spatial distribution would make it difficult to detect global trends. Additionally, the decrease in solar radiation is likely due to the burning of coal, oil and wood, power stations, and other atmospheric pollutants. These pollutants compel a part of solar energy to be reflected back out to space, and this cooling effect is believed to have counteracted part of the greenhouse gas warming effect. The MBD values between re-analysis and measurements of global solar radiation were less than 4 MJ m^{-2} day^{-1}, while NRMSD was 0.7%. The reason for these errors could be related to the increasing cloudiness resulting from the high flux of water vapor to the atmosphere by large irrigation in the region, once clouds play an important role in modifying radiation.

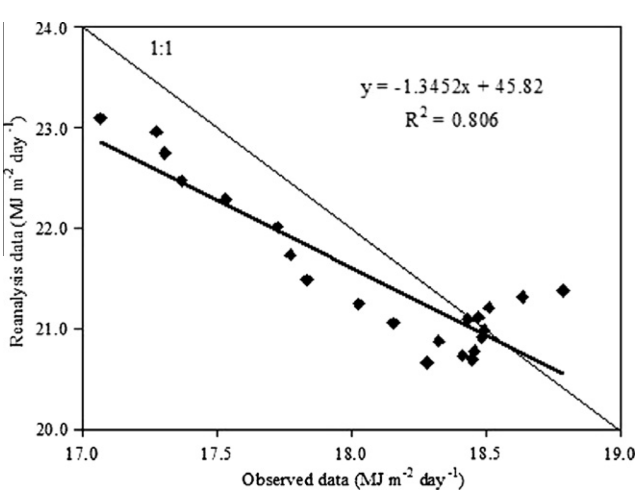

Fig. 6. Relationship between re-analysis and measurements data at grid point 46 (mean values for Petrolina and Juazeiro stations) of global solar radiation (MJ m^{-2} day^{-1}).

3.4. Trends in global radiation

The least-square method was also applied to the net radiation, shortwave and longwave from NCEP/NCAR database in four select grid points over northeastern Brazil, after excluding cycles (Fig. 7). The slopes of regression lines indicated that for all grids both shortwave and longwave radiation were decreasing while net radiation was increasing. Therefore, only a small part of the change in net radiation was due to the longwave radiation. With the exception of net radiation at grid 34, the time series did not present any statistically significant trend. On average, longwave and shortwave represented 28.8% and 72.2% of the net radiation, respectively. Grids 18 and 34 are located over the continent, while grids 69 and 72 are located over the Atlantic Ocean on the northern and southern parts, respectively. The mean values of longwave, shortwave and net radiation were observed to be lower over the continent than over the Atlantic Ocean. A possible reason for this can be attributed to the environmental impacts of anthropogenic activities changing the surface albedo. Results also showed that for long-time periods, the longwave radiation was less variable than shortwave and net radiation.

Simple regression was done for the time series of global solar radiation from NCEP/NCAR re-analysis data without decadal cycles for determining the slopes of the regression lines per period and the corresponding significance p-level. Fig. 8 depicts the spatial distribution of annual mean daily global solar radiation trends over the studied region and its significance p-level. The highest values in global solar radiation were found in the central part of northeastern Brazil exactly over the semiarid region where the rainfall is less than 400 mm per year and annual evaporation overcomes 2000 mm (Silva et al., 2010). On the other hand, the lowest values were obtained in the northeast part of study region due to high cloudiness which usually comes from the Amazon region (Fig. 8a). There was a decreasing trend in global solar radiation from NCEP/NCAR re-analysis data just in some extensive area located in the semiarid region (Fig. 8b). Most of these trends were statistically significant at the $p < 0.05$ level according to the Mann–Kendall test. The possible cause of reduction in solar radiation is associated with the increase in air pollutants, which have changed the optical properties of atmosphere

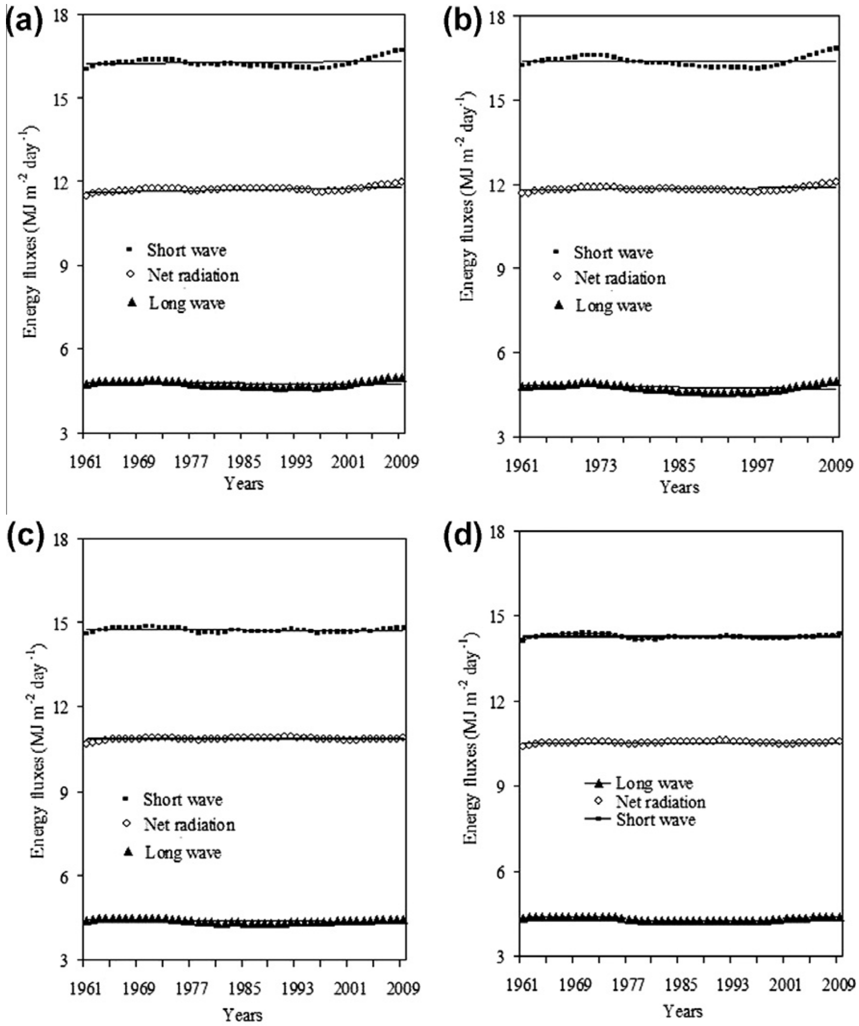

Fig. 7. Long-term trends in shortwave, longwave and net radiation for grid point 34 (a); grid point 18 (b); grid point 69 (c) and grid point 72 (d).

components, particularly those provided by cloudiness (Stanhill and Cohen, 2001). For the whole period of analysis, trends in annual average daily global solar radiation varied from −2.8 to 1.5 MJ m^{-2} day^{-1}. Mean and coefficient of variation of the solar radiation variables for each group in northeastern Brazil are given in Table 4. Annual mean daily solar radiation ranged from 18.8 MJ m^{-2} day^{-1} for group 2 to 21.4 MJ m^{-2} day^{-1} for group 1, with a mean of 20.3 MJ m^{-2} day^{-1} for the whole study region.

On average, surface net radiation represented 49.8% of the global solar radiation while the net longwave radiation and net radiation represented 30.4% and 69.6% of net shortwave radiation. The highest variability in global solar radiation occurred for group 2, while the lowest was observed for group 4. The net shortwave radiation showed the highest variability among radiation variables up to 31.2% for group 3. This result may be due to the fact that the cloud cover in group 2 was partially controlled by Intertropical Convergence Zone which is quite irregular throughout the year. On the other hand, the cloudiness was more homogenous in group 4 because of the regular occurrence of cold fronts throughout the year.

Since data from well-calibrated pyranometers and heliographs are scarce and seldom available over extended regions, solar radiation data from NCEP/NCAR re-analysis can be used in many solar energy applications. This result is important to the solar power as a suitable source of energy, because of the high solar radiation available in many developing countries, like Brazil, and the low maintenance requirements. The interest in solar powers has also increased in other parts of the world because of the need for more environmental friendly power generation to attend to both the future power demand and the survival of our planet (Ehnberg and Bollen, 2005). The main disadvantage of the NCEP/NCAR data is the lack of spatial resolution. Another important disadvantage of the re-analysis data is its low accuracy with regard to radiative variables. Also, trends in tropospheric aerosol are not present in the re-analysis data, and clouds, which have the highest impact on surface solar radiation, are poorly simulated by the NCEP model. However, re-analysis data incorporate at least some of the observed climate variability, particularly the decadal cycles. The reduction in sunlight or global solar radiation means that less water is evaporated from the

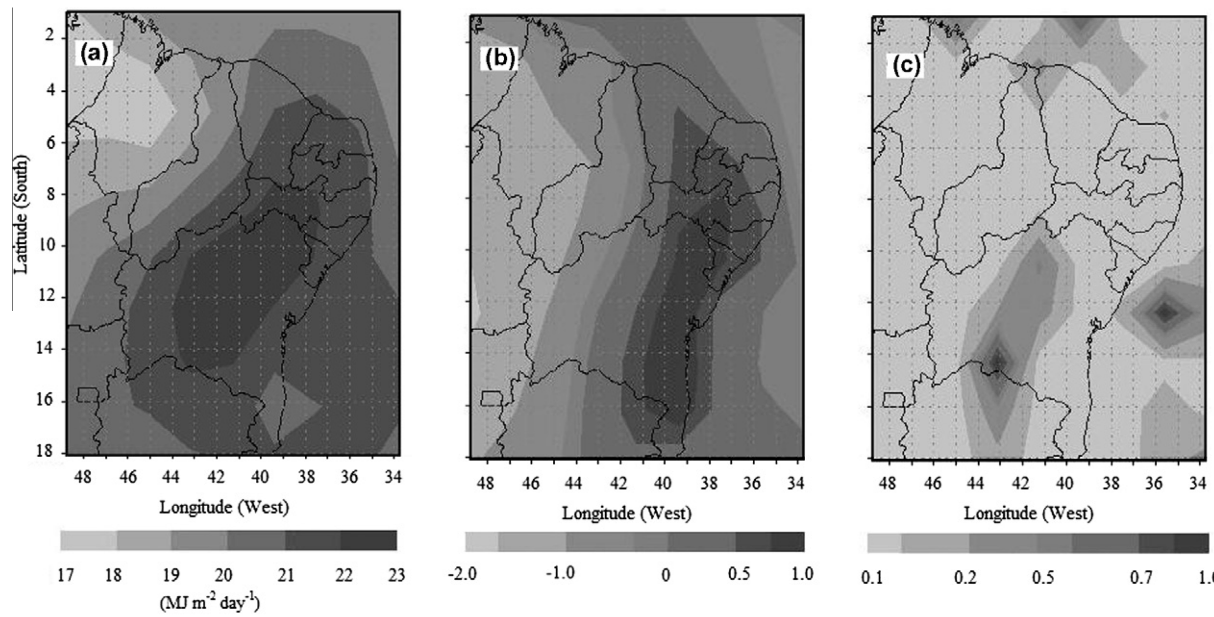

Fig. 8. Spatial distribution of long-term average in global solar radiation (a), trends in solar radiation (b) and corresponding *p*-level (c) in northeastern Brazil for the 1948–2009 period. Slopes of the annual global solar radiation (MJ m^{-2} day^{-1}) linear regression for the corresponding time period are expressed per analyzed period (1962–2009).

Table 4
Mean values and coefficient of variation (CV, %) of solar radiation variables (MJ m^{-2} day^{-1}) for each group in northeastern Brazil.

Groups	Net radiation		Global solar radiation		Longwave		Shortwave	
	Mean	CV	Mean	CV	Mean	CV	Mean	CV
Group 1	11.2	4.1	21.4	4.2	4.7	4.2	15.9	4.9
Group 2	11.6	1.2	18.8	6.1	4.7	2.6	16.3	1.6
Group 3	8.4	28.4	19.9	2.9	4.0	19.1	12.3	31.2
Group 4	9.2	14.7	21.0	1.7	4.2	11.0	13.4	16.3
Average	10.1	12.1	20.3	3.72	4.4	9.2	14.5	13.5

oceans, lakes or rivers. Most of this reduction is clearly linked to the global dimming resulting in a less efficient water cycle in the earth-atmosphere system. These are consistent with the fact that the earth's warming due to the CO_2 increase and natural variations over the past century.

4. Conclusions

Annual and monthly averaged NCEP/NCAR re-analysis and measured data on solar radiation from 1958 to 2009 and measured sunshine duration for distinct periods are used for assessing global dimming in northeastern Brazil. The effects of decadal and multi-decadal cycles are removed from the data through the use of a moving average technique, and the results demonstrate the existence of consistent and statistically significant trends in the observed and modeled global solar radiation data. Modeled global solar radiation values are in satisfactory agreement with the sunshine duration in northeastern Brazil. The coefficient of determination vary from 0.49 in group 3 to 0.77 in group 2 indicate reasonable correlation between global solar radiation from NCEP/NCAR re-analysis and data collection platform (DCP) data. Results also showed that there is an agreement in trend or inter-annual variability between re-analysis and measured global solar radiation. Despite the re-analysis, surface radiation fluxes have no input from actual observations, and there is evidence to believe that the re-analysis surface radiation flux data trends have correspondence to the reality.

Both solar global radiation measurements and radiation data from NCEP/NCAR re-analysis project provide consistent evidence of the global dimming effect over northeastern Brazil. Statistically significant alterations in solar radiation and sunshine duration over the region may be due to the changes in atmospheric optical properties. However, further measurements in solar radiation for the studied region are necessary for getting a data set enough homogenous to compare with that derived from NCEP/NCAR database. The main findings of this study are the detected reductions in global solar radiation in the semiarid region of northeastern Brazil and the agreement between re-analysis and DCP data. As described in the NCEP re-analysis, surface fluxes are a class "C" variable in the re-analysis product (Kalnay et al., 1996), meaning that they are largely based on model returns and not constrained by data. Therefore, there are possible uncertainties in the reanalysis trends for any points of the studied region.

References

Abakumova, G.M., Feigelson, E.M., Russak, V., Stadnik, V.V., 1996. Evaluation of long-term changes in radiation, cloudiness, and surface temperature on the territory of the former Soviet Union. J. Climate 9, 1319–1327.

Bakirci, K., 2009. Correlations for estimation of daily global solar radiation with hours of bright sunshine in Turkey. Energy 34, 485–501.

Chen, J., Carlson, B.E., Del Genio, A.D., 2002. Evidence for strengthening of the tropical general circulation in the 1990s. Science 295, 838–841.

Chineke, T.C., 2008. Equations for estimating global solar radiation in data sparse regions. Renew. Energy 33, 827–831.

Gueymard, C.A., Myers, D.R., 2009. Evaluation of conventional and high-performance routine solar radiation measurements for improved solar resource, climatological trends, and radiative modeling. Sol. Energy 83, 171–185.

Fotiadi, A., Hatzianastassiou, N., Matsoukas, C., Pavlakis, K.G., Drakakis, E., Hatzidimitriou, D., Vardavas, I., 2005. Analysis of the decrease in the tropical mean outgoing shortwave radiation at the top of atmosphere for the period 1984–2000. Atmos. Chem. Phys. 5, 1721–1730.

Davis, J.C., 1986. Statistics and Data Analysis in Geology. Wiley, New York, 646 pp.

Ehnberg, J.S.G., Bollen, M.H.B., 2005. Simulation of global solar radiation based on cloud observations. Sol. Energy 78, 157–162.

El-Metwally, M., 2004. Simple new methods to estimate global solar radiation based on meteorological data in Egypt. Atmos. Res. 69, 217–239.

El-Metwally, M., 2005. Sunshine and global solar radiation estimation at different sites in Egypt. J. Atmos. Terr. Phys. 67, 1331–1342.

Eskridge, R.E., Ku, J.Y., Rao, S.T., Porter, P.S., Zurbenko, I.G., 1997. Separating different scales of motion in time series of meteorological variables. Bull. Am. Meteorol. Soc. 78, 1473–1483.

Gore Jr., P.A., 2000. Handbook of Applied Multivariate Statistics and Mathematical Modeling, p. 321.

Grimm, A.M., 2003. The El Niño impact on the summer monsoon in Brazil: regional processes versus remote influences. J. Climate 16, 263–280.

Hatzidimitriou, D., Vardavas, I., Pavlakis, K., Hatzianastassiou, N., Matsoukas, C., Drakakis, E., 2004. On the decadal increase in the tropical mean outgoing longwave radiation for the period 1984–2000. Atmos. Chem. Phys. 4, 1419–1425.

Hirsch, R.M., Slack, J.R., Smith, R.A., 1982. Techniques of trend analysis for monthly water quality data. Water Resour. Res. 18, 107–121.

Kalnay, E., Kanamitsu, M., Kistler, R., Collins, W., Deaven, D., Gandin, L., Iredell, M., Saha, S., White, G., Woollen, J., Zhu, Y., Chelliah, M., Ebisuzaki, W., Higgins, W., Janowiak, J., Mo, K.C., Ropelewski, C., Wang, J., Leetmaa, A., Reynolds, R., Jenne, R., Joseph, D., 1996. The NCEP/NCAR 40-year reanalyses projects. Bull. Am. Meteorol. Soc. 77, 437–471.

Kayano, M.T., Andreoli, R.V., 2004. Decadal variability of northern northeast Brazil rainfall and its relation to tropical sea surface temperature and global sea level pressure anomalies. J. Geophys. Res. 109. doi:10.1029/2004JC002429.

Kayano, M.T., Andreoli, R.V., 2007. Relations of south American summer rainfall interannual variations with the Pacific Decadal Oscillation. Int. J. Climatol. 27, 531–540.

Kendall, M.G., 1975. Rank Correlation Measures. Charles Griffin, p. 220.

Yu, P.S., Yang, T.C., Wu, C.K., 2002. Impact of climate change on water resources in southern Taiwan. J. Hydrol. 260, 161–175.

Liepert, B.G., Kukla, G.J., 1997. Decline in solar radiation with increased horizontal variability in Germany between 1964 and 1990. J. Climate 10, 2391–2401.

Liepert, B.G., 2002. Observed reductions of surface solar radiation at sites in the United States and worldwide from 1961 to 1990. Geophys. Res. Lett. 29. doi:10.1029/2002GL014910.

Liu, B., Xu, B., Henderson, M., Gong, W., 2004. A spatial analysis of pan evaporation trends in China, 1955–2000. Geophys. Res. Lett. 109. doi:10.1029/2004JD004511.

Lohmann, S., Schillings, C., Mayer, B., Meyer, R., 2006. Long-term variability of solar direct and global radiation derived from ISCCP data and comparison with reanalysis data. Sol. Energy 80, 1390–1401.

Mann, H.B., 1945. Nonparametric tests against trend. Econometrica 13, 245–259.

Nazarenko, L., Menon, S., 2005. Varying trends in surface energy fluxes and associated climate between 1960 and 2002 based on transient climate simulations. Geophys. Res. Lett. 32. doi:10.1029/2005GL024089.

Power, H.C., Goyal, A., 2003. Comparison of aerosol and climate variability over Germany and South Africa. Int. J. Climatol. 23, 921–941.

Power, H.C., Mills, D.M., 2005. Solar radiation climate change over South Africa and an assessment of the radiative impact of volcanic eruptions. Int. J. Climatol. 25, 295–318.

Silva, V.P.R., 2004. On climate variability in Northeast of Brazil. J. Arid Environ. 58, 575–596.

Silva, V.P.R., Sousa, F.A.S., Cavalcanti, E.P., Souza, E.P., Silva, B.B., 2006. Teleconnections between sea-surface temperature anomalies and air temperature in northeast Brazil. J. Atmos. Sol. – Terr. Phys. 68, 781–792.

Silva, V.P.R., Campos, J.H.C., Azevedo, P.V., 2009. Water-use efficiency and evapotranspiration of mango orchard grown in northeastern region of Brazil. Sci. Horticult. 120, 467–472.

Silva, V.P.R., Azevedo, P.V., Brito, R.S., Campos, J.H.B.C., 2010. Evaluating the urban climate of a typically tropical city of northeastern Brazil. Environ. Monit. Assess. 161, 45–59. doi:10.1007/s10661-008-0726-3.

Stanhill, G., Cohen, S., 2001. Global dimming: a review of the evidence for a widespread and significant reduction in global radiation with discussion of its probable causes and possible agricultural consequences. Agric. Forest Meteorol. 107, 255–278.

Supit, I., Van Kappel, R.R., 1998. A simple method to estimate global radiation. Sol. Energy 63, 147–160.

Tashima, D.H., Hartmann, D.L., 1998. Regional trends in Nimbus-7 OLR: effects of a spectrally nonuniform albedo. J. Climate 12, 1458–1466.

Vera, C., Silvestri, G., Barros, V., Carril, A., 2004. Differences in El Niño response over the southern hemisphere. J. Climate 17, 1741–1753.

Zarzalejo, L.F., Polo, J., Martín, L., Ramírez, L., Espinar, B., 2009. A new statistical approach for deriving global solar radiation from satellite images. Sol. Energy 83, 480–484.

Yang, K., Huang, G.W., Tamai, N., 2001. A hybrid model for estimating global solar radiation. Sol. Energy 70, 13–22.

Wan, K.K.W., Cheung, K.L., Liu, D., Lam, J.C., 2009. Impact of modeled global solar radiation on simulated building heating and cooling loads. Energy Convers. Manage. 50, 662–667.